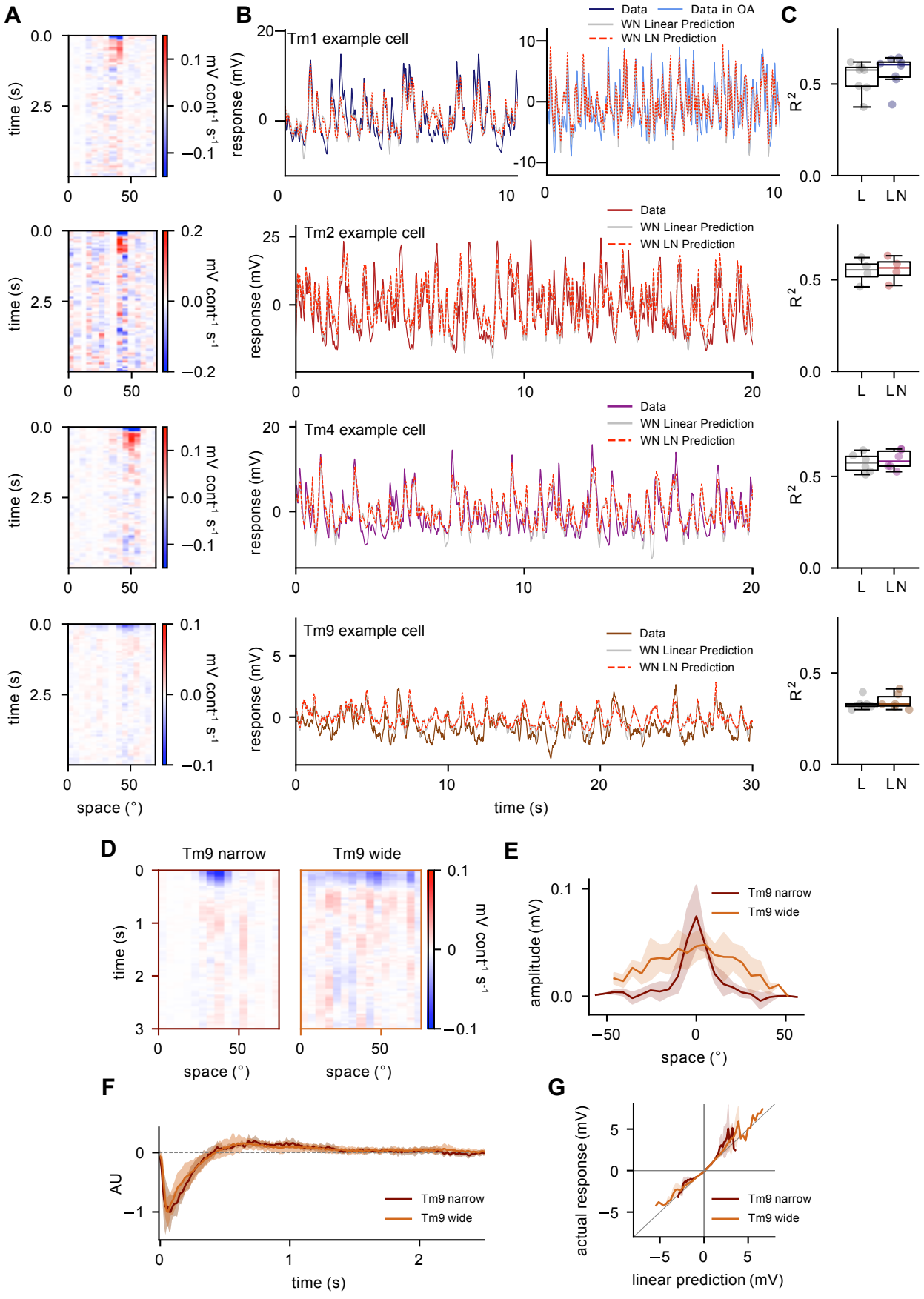
A
B
C
time (s)
space (°)
mV cont⁻¹ s⁻¹
response (mV)
time (s)
Data
Data in OA
WN Linear Prediction
WN LN Prediction
Tm1 example cell
Tm2 example cell
Tm4 example cell
Tm9 example cell
R²
L
LN
D
Tm9 narrow
Tm9 wide
space (°)
time (s)
mV cont⁻¹ s⁻¹
E
amplitude (mV)
space (°)
F
AU
time (s)
G
actual response (mV)
linear prediction (mV)

**Figure S1: White Noise Analysis and Tm9 Variability. Related to Figure 2. A.** Example white noise spatiotemporal linear filters extracted for single Tm1, Tm2, Tm4 and Tm9 neurons. **B.** Comparison of raw data (colored line), white noise filter linear prediction (grey line) and the white noise filter linear-nonlinear (LN) prediction (dashed red line) for the same neurons as in A. **C.** $R^2$ values are comparable between linear and linear-nonlinear (LN) predictions for all cells. **D.** Example spatiotemporal receptive fields for narrow (n=6) and wide (n=8) Tm9 cells **E.** Narrow and wide spatial receptive fields (FWHM=15.4°, FWHM=60.3° when fit with a Gaussian) **F.** Temporal filters do not significantly differ **G.** Static nonlinearities do not significantly differ.

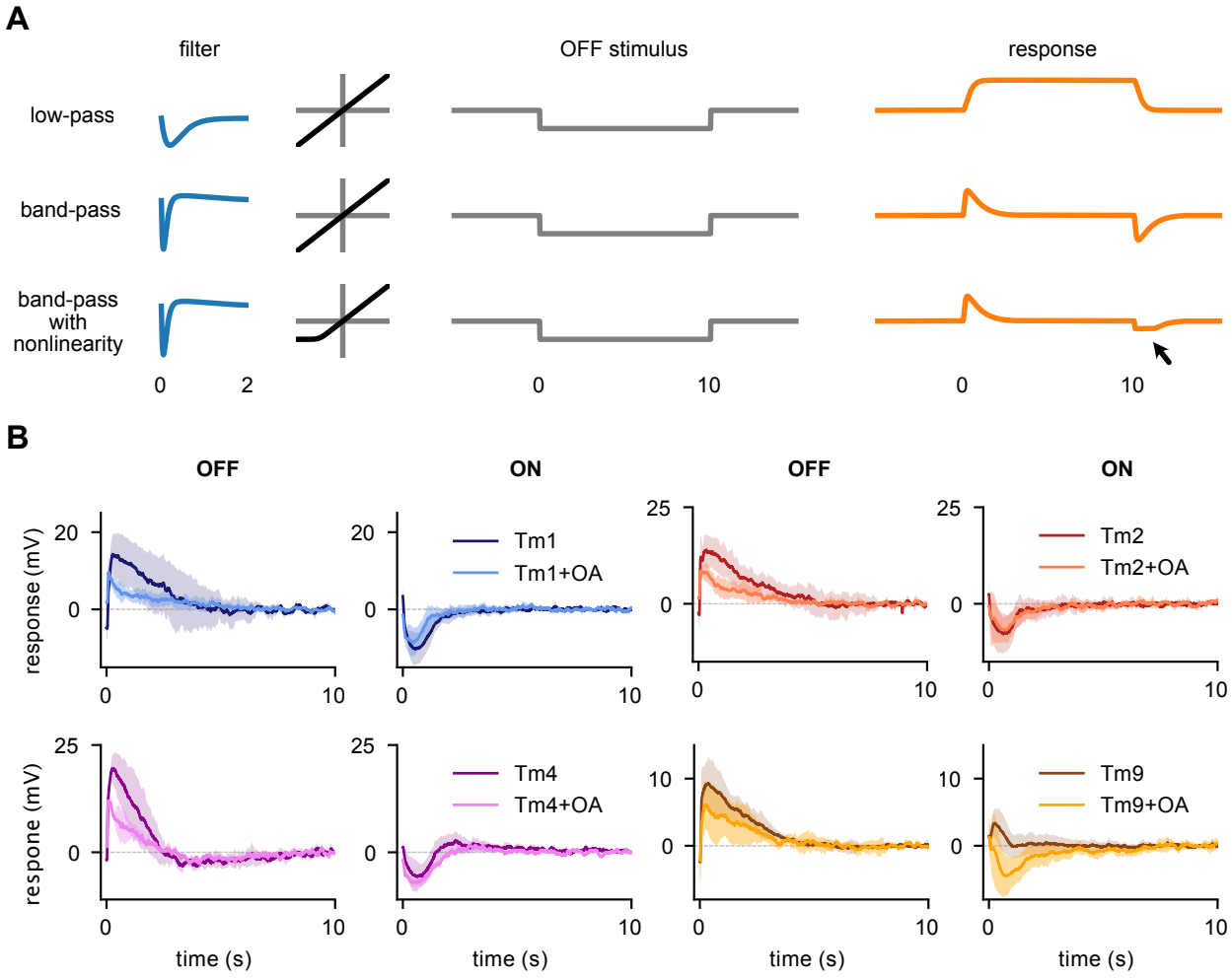


**Figure S2: Long OFF and ON responses exhibit band-pass properties and are partially rectified. Related to Figure 2. A.** A low-pass filter (*top*) produces a response that fails to return to baseline until the stimulus ends, while a band-pass filter produces a response that returns to baseline during the course of a long stimulus. A linear band-pass filter produces symmetric responses to OFF and ON stimuli (*middle*), while a partially rectified band-pass filter produces asymmetric response to OFF and ON stimuli (*bottom*) **B.** Tm1 (n=4 saline, n=4 OA), Tm2 (n=6, n=4), Tm4 (n=4, n=2) and Tm9 (n=11, n=10) responses to 10 s OFF flashes and 10 s ON flashes in saline and in OA. All four neurons return to baseline during the flashes and therefore exhibit band-pass properties. They all show partial rectification in their ON responses. Tm9s presented more variability in their responses, with some cells showing depolarizing ON responses, resulting in depolarizing ON average.

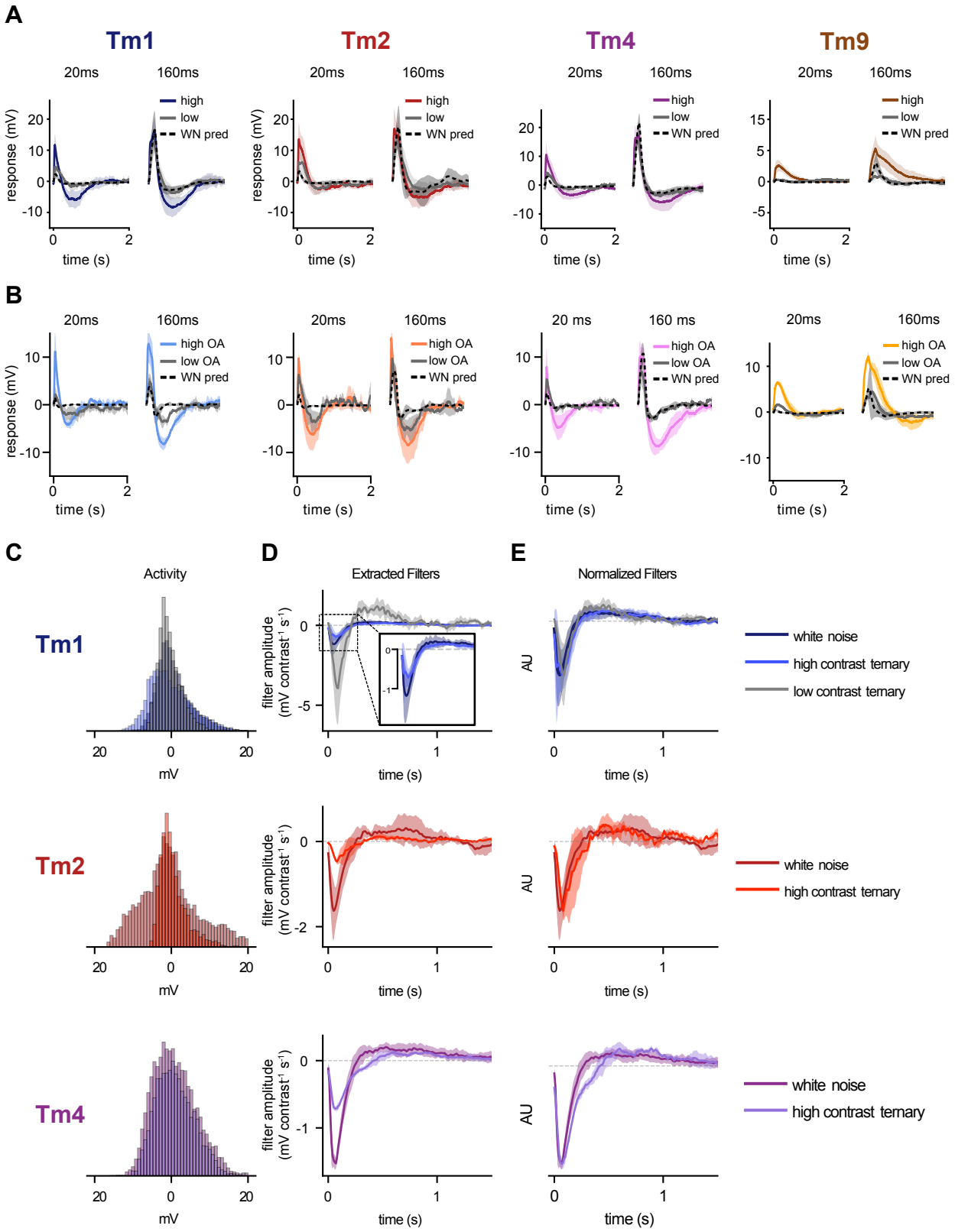
A
Tm1
Tm2
Tm4
Tm9
20ms
160ms
high
low
WN pred
response (mV)
time (s)
B
high OA
low OA
20 ms
C
Activity
mV
D
Extracted Filters
filter amplitude (mV contrast⁻¹ s⁻¹)
E
Normalized Filters
AU
white noise
high contrast ternary
low contrast ternary

**Figure S3: Signal statistics drive the shape changes in the response of T5 inputs. Related to Figure 3. A.** Mean Tm responses to 20 ms and 160 ms low contrast (grey) and high contrast flashes (color, same data as in B). Low contrast flashes do not elicit biphasic responses and are closer in shape to white noise predictions from A. Tm1 (n=5), Tm2 (n=4-5), Tm4 (n=2), and Tm9 (n=1-2). **B.** Tm1, Tm2, Tm4 and Tm9 responses to flashes of high vs. low contrast (n=4, n=3, n=2, n=2, respectively) in the presence of OA. OA white noise filter predictions superimposed (black dashed line). **C.** Histogram of response values across white noise, high contrast ternary noise, and low contrast ternary noise conditions. Different conditions elicit responses in the same general dynamic range, although low contrast responses overall have slightly lower amplitude **D.** Average temporal filters extracted from truncated white noise ($\mu = 0$, $\sigma = 1$, truncated at $\pm 1$, same data as in Figure 2A), high contrast ternary noise (values randomly selected from $+1$, $-1$ and 0) for Tm1 (n=4), Tm2 (n=2) and Tm4 (n=2), and low contrast ternary noise (values randomly selected from $+0.1$, $-0.1$ and 0) for Tm1 (n=4). Filter amplitude differences indicate gain adaptation so that response of cell is within similar dynamic range regardless of contrast. While this is especially evident in the case of the low contrast ternary noise-extracted Tm1 filter (*top*, grey trace), the same effect can be seen between high contrast ternary noise and the white noise (lower contrast)-extracted filters for Tm1 (*inset*), Tm2, and Tm4. **E.** When scaled, filters do not show strong differences in shape.

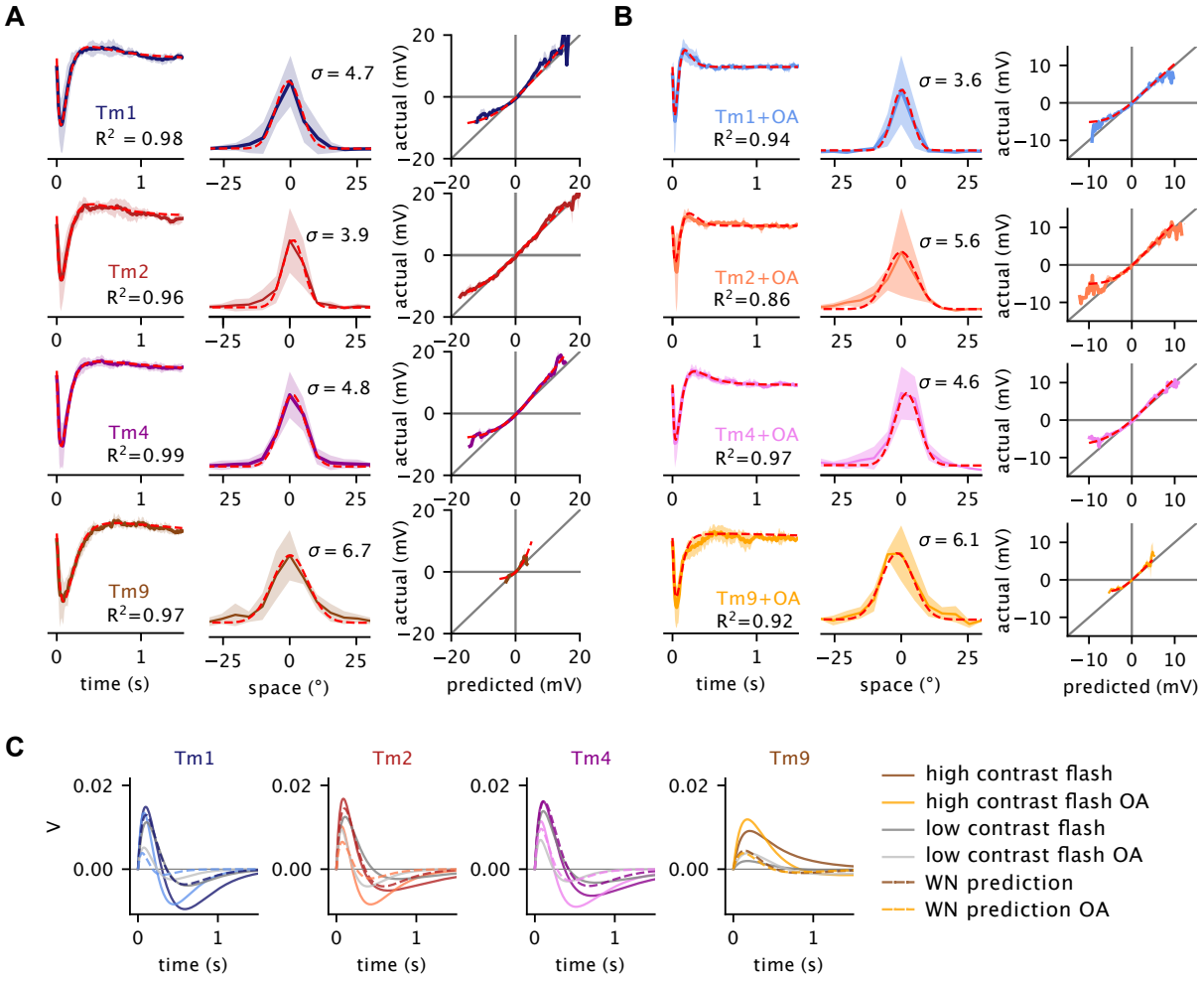


**Figure S4: Paramaterization of white noise filters and flash data. Related to Figure 4. A.** Parameterization of white noise temporal filters (*left*), spatial filters (*middle*), and static nonlinearities (*right*). Same traces as in Figure 2, with parameterization superimposed (red dashed line) **B.** Same for OA, with traces from Figure 2. **C.** Comparison of parameterized Tm1, Tm2, Tm4 and Tm9 responses to 160 ms flashes across conditions, including high contrast and high contrast with OA (solid colored lines), low contrast and low contrast with OA (grey lines), and both baseline and OA LN white noise filter predictions for 160 ms stimuli (dashed lines). These parameterized fits are used in Figure 4A, B.

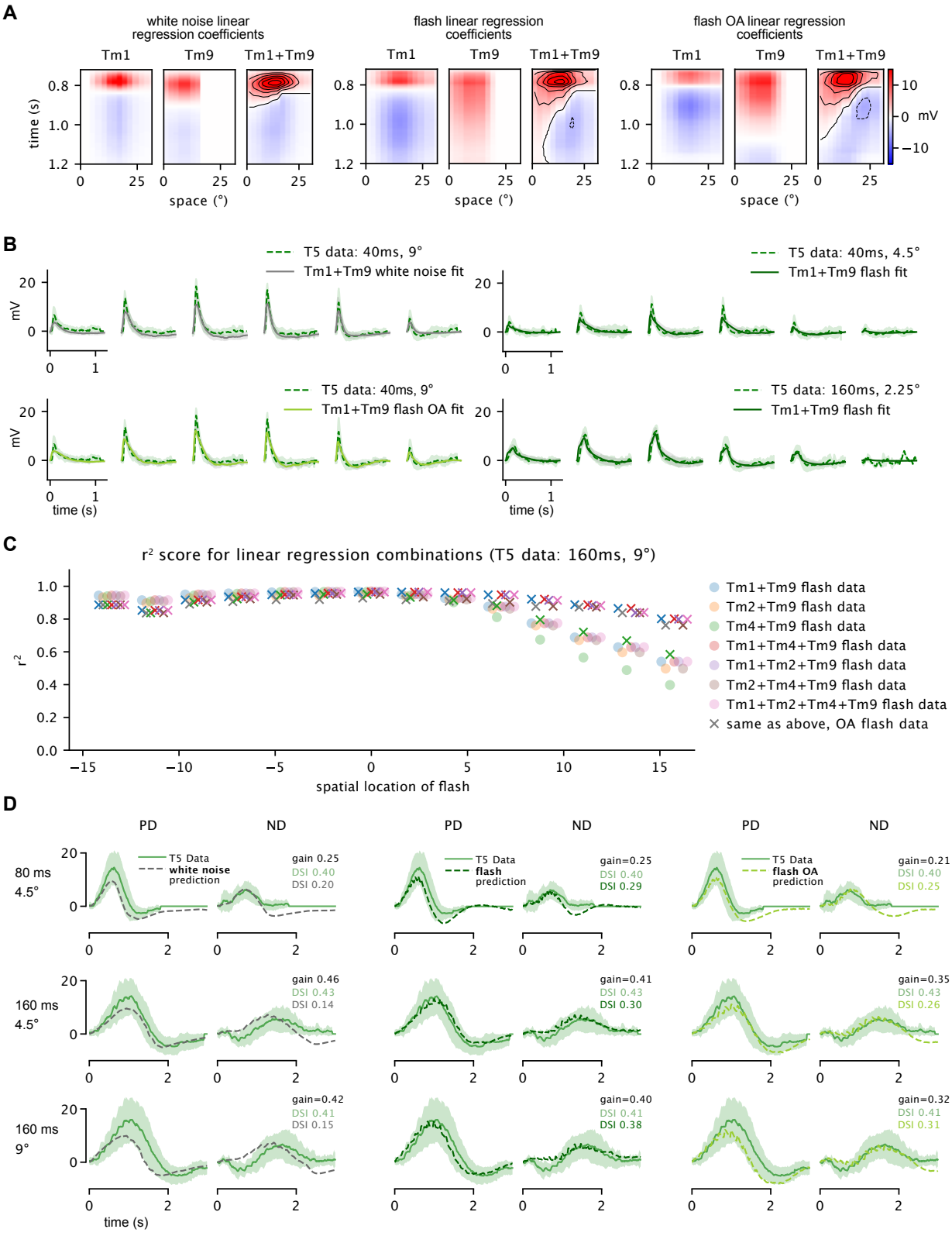
A
white noise linear regression coefficients
flash linear regression coefficients
flash OA linear regression coefficients
Tm1
Tm9
Tm1+Tm9
time (s)
space (°)
mV
B
T5 data: 40ms, 9°
Tm1+Tm9 white noise fit
T5 data: 40ms, 4.5°
Tm1+Tm9 flash fit
T5 data: 40ms, 9°
Tm1+Tm9 flash OA fit
T5 data: 160ms, 2.25°
Tm1+Tm9 flash fit
mV
time (s)
C
r² score for linear regression combinations (T5 data: 160ms, 9°)
r²
spatial location of flash
Tm1+Tm9 flash data
Tm2+Tm9 flash data
Tm4+Tm9 flash data
Tm1+Tm4+Tm9 flash data
Tm1+Tm2+Tm9 flash data
Tm2+Tm4+Tm9 flash data
Tm1+Tm2+Tm4+Tm9 flash data
same as above, OA flash data
D
PD
ND
80 ms
4.5°
160 ms
4.5°
160 ms
9°
T5 Data
white noise prediction
flash prediction
flash OA prediction
gain 0.25
DSI 0.40
DSI 0.20
gain=0.25
DSI 0.40
DSI 0.29
gain=0.21
DSI 0.40
DSI 0.25
gain 0.46
DSI 0.43
DSI 0.14
gain=0.41
DSI 0.43
DSI 0.30
gain=0.35
DSI 0.43
DSI 0.26
gain=0.42
DSI 0.41
DSI 0.15
gain=0.40
DSI 0.41
DSI 0.38
gain=0.32
DSI 0.41
DSI 0.31
time (s)

**Figure S5: Extended linear regression analysis. Related to Figure 5. A.** Four examples of linear regressions from individual stimulus conditions varying in the length of stimulation (40 ms and 160 ms), as well as bar width (9°, 4.5°, and 2.25°). T5 data from Gruntman et al.[S1]. **B.** In Figure 5, we chose to apply linear regression with Tm1 and Tm9. Combinations of Tm1, Tm2, and Tm4 with Tm9 perform approximately equally well (saline fits shown in circles, OA fits shown with crosses). **C.** Tm1 and Tm9 weighted by linear regression coefficients at each spatial location in the 160 ms, 9° condition, for the three fits enumerated in Figure 5 (using white noise filter predictions, flash responses, and flash OA responses, see Methods). The weighted Tm1 and Tm9 components are summed to generate a representative spatiotemporal receptive field (*right of each panel*). **D.** Gruntman et al.[S1] recorded T5 responses to moving bars across multiple stimulus conditions (20, 40, 80, and 160 ms duration and 2.25°, 4.5°, and 9° bar width). Linear regression coefficients fit to static flashes across conditions (160 ms, 4.5° and 9°) predict T5 moving bar temporal responses (see Methods). In particular, the Tm1 and Tm9 flash data in the baseline saline condition and OA condition match the T5 electrophysiology traces, as well as DSI (*center column, right column*). Note that both PD and ND traces are scaled by a single "gain" factor (see Methods).

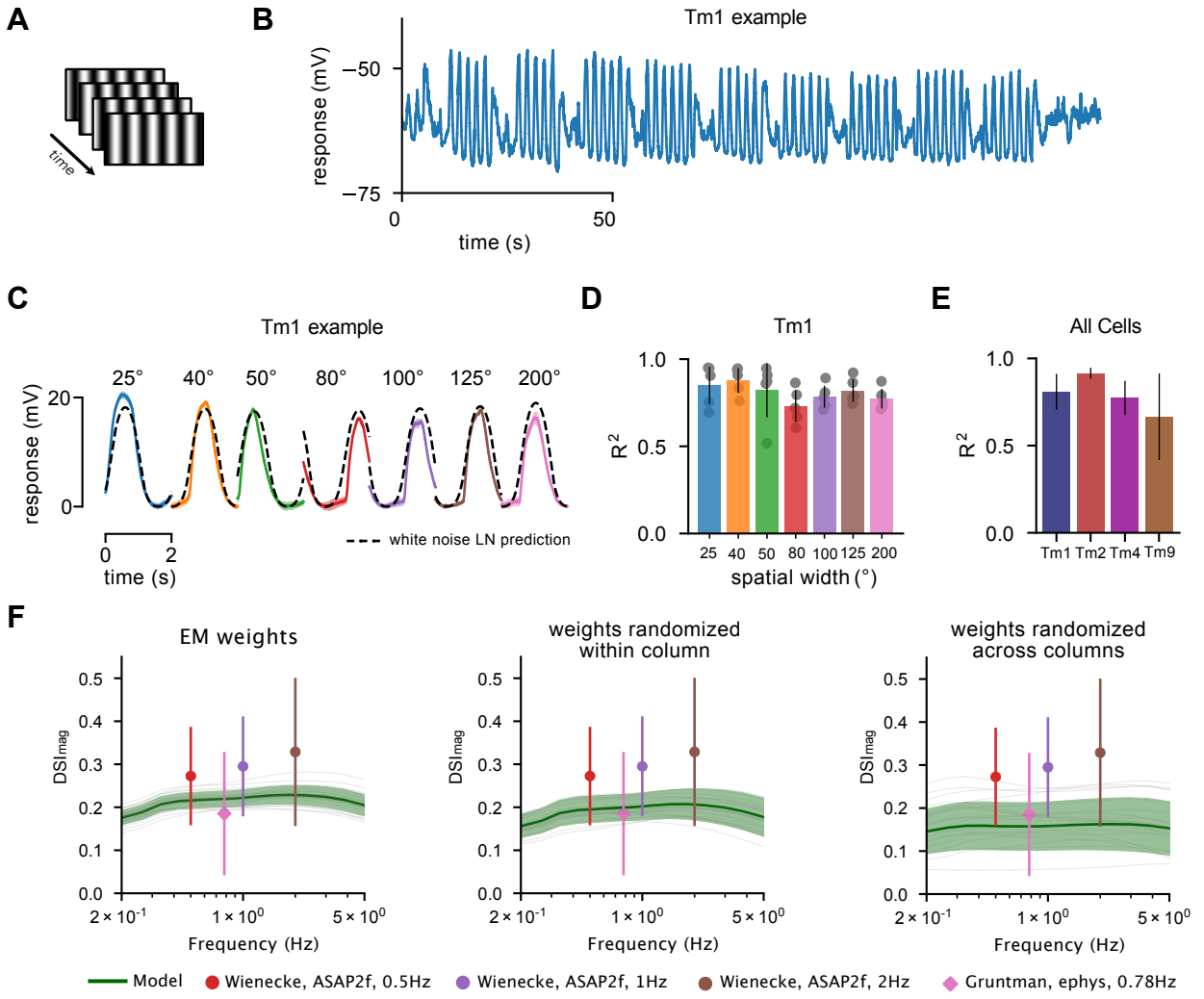


**Figure S6: Drifting grating responses are well predicted by white noise filters, EM weights produce best model performance. Related to Figure 6. A.** Drifting gratings with 0.5 Hz temporal frequency and with varying spatial frequencies were shown **B.** Raw drifting grating response for example Tm1 cell. Each response segment corresponds to a grating presentation of varying spatial frequencies (in order) 10°, 12.5°, 25°, 40°, 50°, 80°, 100°, 125°, and 200° **C.** Averaged periodic responses for each spatial frequency (colored traces for a single example Tm1 cell). A linear-nonlinear prediction based on the corresponding spatiotemporal white noise filter captures the temporal aspects of the response (dashed black line). **D.** $R^2$ responses for each stimulus condition across Tm1 cells (n=5). The match between predicted and actual responses indicates that using a white noise filter linear-nonlinear framework to model T5 responses to drifting gratings is reasonable. **E.** $R^2$ responses for Tm1 (n=5), Tm2 (n=1), Tm4 (n=2) and Tm9 (n=3) averaged across stimulus conditions. **F.** Predicted T5 output using EM weights (*left, same data as in Figure 6C*) has higher DSI, and performs more similarly to recorded T5 responses from Wienecke et al.[S2] and Gruntman et al.[S1] than predicted output using EM weights randomized within column (i.e. Tm1, Tm2 and Tm4, with Tm9 fixed at 0.45 *middle*) or EM weights that have been randomized completely (i.e. Tm1, Tm2, Tm4 and Tm9, *right*, see Methods).

# References

S1. E. Gruntman, S. Romani, M. B. Reiser, The computation of directional selectivity in the *Drosophila* off motion pathway, Elife 8 (2019) e50706.

S2. C. F. Wienecke, J. C. Leong, T. R. Clandinin, Linear summation underlies direction selectivity in *Drosophila*, Neuron 99 (2018) 680–688.